ANALYTICAL AND EXPERIMENTAL CYCLIC RESPONSE OF RC WALLS WITH SETBACK DISCONTINUITIES

I. Manríquez [(1)], S. Díaz [(1)], L. M. Massone [(2)], F. Rojas [(3)], R. Herrera [(3)]

[(1)] *Graduate, Department of Civil Engineering, University of Chile*
[(2)] *Associate Professor, Department of Civil Engineering, University of Chile, lmassone@ing.uchile.cl*
[(3)] *Assistant Professor, Department of Civil Engineering, University of Chile*

Abstract

Chile concentrates a high number of earthquakes along its history. One of the strongest in recent years was in the south of the country, specifically in Maule regions in February, 2010 (8.8 Mw). Several buildings of the modern construction presented damage in reinforced concrete (RC) walls (crushing of concrete, buckling and fracture of steel reinforcement); this was due to little or no confinement used in the design. Other characteristics that are common in damage walls was the relatively high axial load, thin walls, as well as, discontinuities in the walls.

Slender RC walls are often used in Chile and commonly, due to architectural constrain, the length of walls changes between floors designated for parking space and upper floors, presenting wall extensions in the upper levels and creating a setback. Similar situation are observed in other cases, but as extensions for walls oriented in an opposite direction. These types of elements are commonly called flag walls. The level of discontinuity has not been treated experimentally and therefore it is necessary to observe its impact in RC walls and compare the results obtained with finite element models used in previous works. Also, the plastic hinge length will be estimated from the test program providing important information for design purposes.

Four structural wall specimens were designed with thickness of 15cm and height of 2,65m. All specimens have a length of 90cm at the base, increasing the length at a specific height for three of them. Two are increased over a length of 25cm and 50cm at a height of 30cm, whereas other specimen increases its length to 25cm, but a height of 60cm. All of them are tested under constant axial stress (0.1f'cAg) and cyclic lateral loads increasing at specific drift levels. The axial load is applied by means of four post-tensioning bars anchored to the wall pedestal. The specimen is fixed to the strong floor and the lateral load is applied with an actuator at the top of the specimen. Main deformation measurements are registered by strain gages on steel bars, LVDTs at the wall surface and photogrammetry to monitor the global response, as well as, local response close to the discontinuity.

The effect of the height and length of the discontinuity will be studied regarding plastic hinge length and maximum compressive and tensile strains in the wall boundary that can lead to damage, and compared with predictive expressions developed in a previous work.

Keywords: slender wall; experiment; flag walls; cyclic loading; discontinuities.

Introduction

On February 27, 2010 Chile was hit by an earthquake of magnitude 8.8 Mw. While infrastructure largely performed well, several modern buildings were damaged in reinforced concrete walls (concrete crushing, buckling and fracture of steel reinforcement); this was due to little or no confinement used in the wall boundary elements, as well as the relatively high axial load, and discontinuities presence in walls. This last aspect has not been reviewed by the Chilean code in its latest version. Due to architectural requirements, the length of walls changes between floors destined for parking, causing an extension of the wall to the upper floors and creating a setback at the edges of the building, commonly referred to as a configuration of flag wall. Fig.1 shows an scheme of wall configuration and damage after the 2010 seismic event.

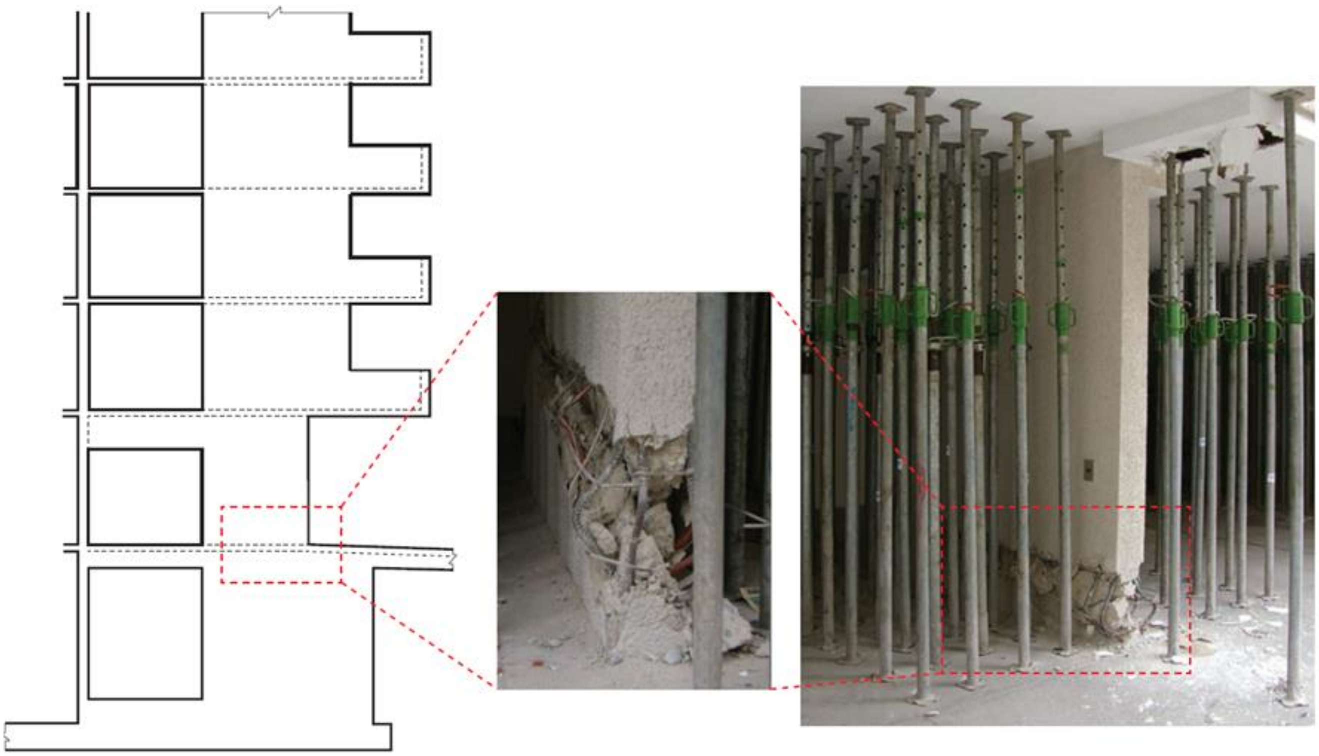

Fig. 1 – Wall damage in discontinuous walls during the 2010 earthquake.

There is investigation in the literature that focus in the response of slender walls with discontinuities. However, most of them have centered their research in door or window openings (i.e., Taylor et al. [4] and Ali and Wight [5]). In order to provide preliminary information on wall setback impact on behavior, the work by Ahumada [2], presents predictive estimation of yield displacement, plastic hinge length and base curvature, based on a fiber model that includes setback at the wall base (flag-wall) as an extension of the work by Massone et al. [1].

In general, the plastic hinge located at the base increases in height as it increases the level of wall top displacement. In the case of rectangular walls, the curvature gradually increases in height, whereas in walls with the presence of discontinuity (setback) at the base, the plastic hinge tends to concentrate at the base. In cases where the height of the discontinuity is larger (taller), behavior is similar to the case of rectangular wall, allowing the plastic hinge to develop. In Fig.2a the first yield point (point in height at which the wall most tensioned fiber yields) develops earlier, that is, at a lower drift level for walls with setback (flag-wall) compared with continuous rectangular walls. Moreover, plastification (hinge) tends to stagnate once the height of the basal discontinuity is achieved (for small discontinuity), suggesting that the entire upper section of the wall tends to behave as a rigid body. Fig.2b shows the curvature values calculated in each layer of elements constituting the flexural model for walls with and without discontinuity. The negative direction is used for the rectangular wall and the positive direction for the wall with discontinuity. The results reveal the concentration of curvature in the last case.

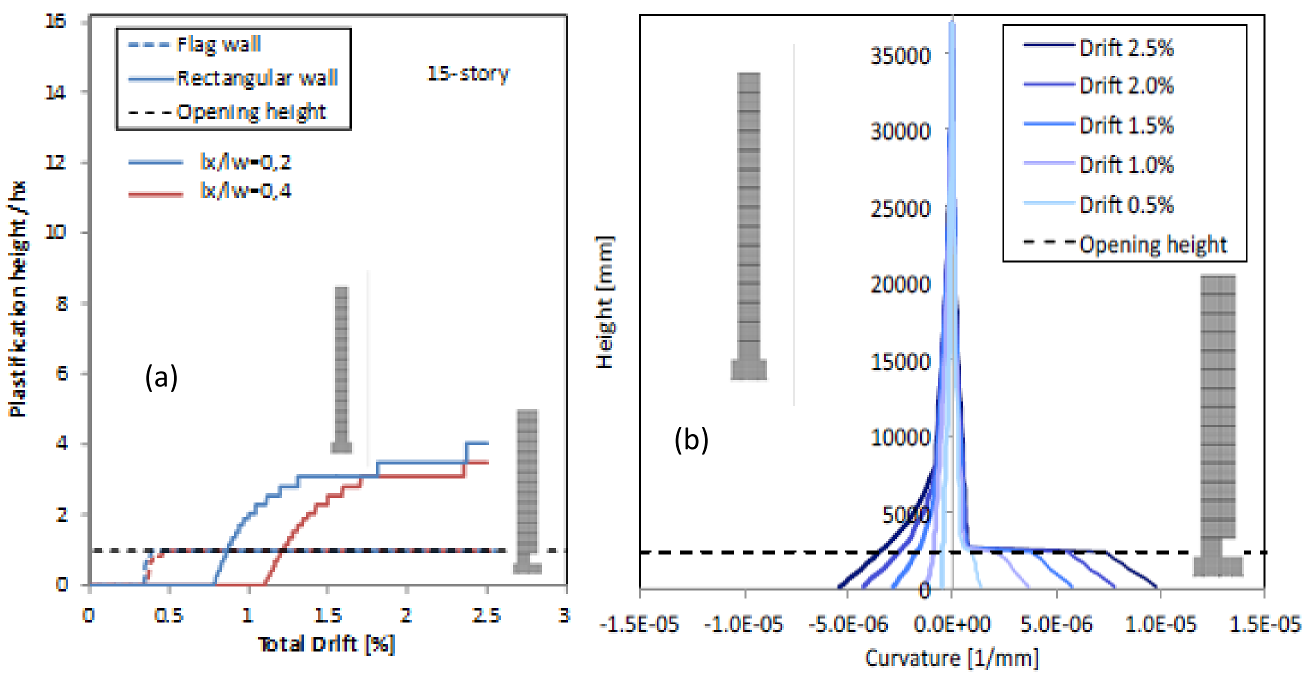

Fig. 2 – Analytical results for a 15-story building [2], (a) Plastification distribution versus drift with discontinuity length of 20% and 40% of the wall length (l_x/l_w); (b) Wall curvature distribution for rectangular and flag-wall for l_x/l_w =0.2 (after Massone et al. [1]).

In this paper, slender reinforced concrete walls with varying degrees of discontinuity at the base are tested. The level of discontinuity in the base has not been treated experimentally and therefore is necessary to observe its structural impact. A comparison between a theoretical study by finite elements and experimental testing reinforced concrete specimens is also performed, as well as comparisons with predictions by previous research [3]. In both cases the effect of the height and length of the discontinuity on the behavior of the plastic hinge formation and the distribution of curvature on its height is observed.

Test program

Fig.3 shows the four reinforced concrete walls specimens, which were designed with a height of 2.65m and 15cm wall thickness. In order to verify the level of discontinuity at the base of these type flag walls, the base Wall was designed with a length of 90 cm (W1), which will be progressively extended in length from a certain height for the 3 remaining specimens. Two specimens have been extended over an additional length of 25cm and 50cm, but only beyond height of 30cm measured from the Wall base (W2 and W3), whereas for the last specimen the length has been increased by 25cm, but beyond height of 60 cm (W4). For the discussion in this

Santiago Chile, January 9th to 13th 2017

article, specimen W4 is left out given the insufficient anchorage of the discontinuous reinforcement. At the top of the wall a concrete beam of 30cm by 40cm is included in order to transmit the applied loads (axial and lateral).

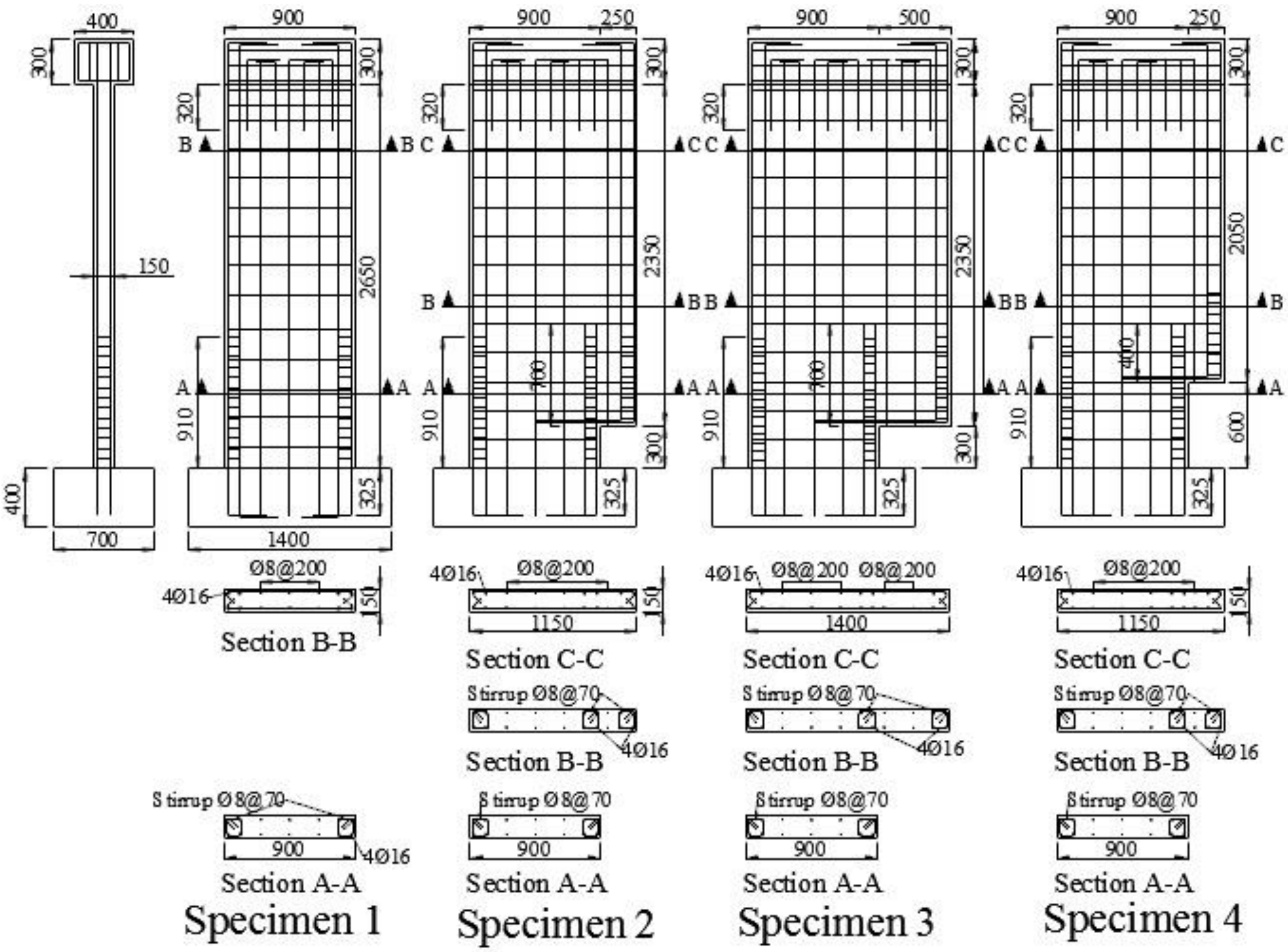

Fig. 3 – Specimens description (units in mm)

Edge reinforcement is formed by 4 bars of $\phi16$ on both sides. It has a confinement made by stirrups $\phi6$ separated each 70 mm, for 1 meter of height. Web of wall is covered by $\phi8$ with separation of 200 mm, in vertical and horizontal direction. All specimens have the same configuration.

Test setup

The specimens are tested similarly as has been done by other authors, such as Taylor et al. [4] and Ali and Wight [5]. The specimens were attached to a strong floor by post-tensioning bars placed at the wall pedestal. Similar attachment was used to fix a lateral actuator to the RC beam placed on the top of the wall. The top beam was restrained to move out-of-plane by means of a Steel frame. Fig. 4 presents a scheme of test setup. All specimens were loaded with axial and lateral loads. The axial compression load was exerted from the upper level of the wall with of magnitude equal to 0.1f'cAg. This was applied through a system of anchored bars to the pedestal base and the load was maintained constant by means of four hydraulic jacks located on a metallic beam in order to better distribute the load.

Besides, the specimens were subjected to cyclic lateral force at 2.8 m height (measured from the wall base) by means of the lateral actuator pinned at both ends, and anchored at the strong wall in one side and the concrete beam on the top of the wall on the other side. This is able to generate up to 100 tons of load and expand approximately 60 cm. The magnitude of cycles increases gradually until reaching the breaking point [6]. The loading level to drift are 0.1%, 0.2%, 0.3%, 0.4%, 0.6%, 0.9%, 1.35%, 2%, 3% and 4%.

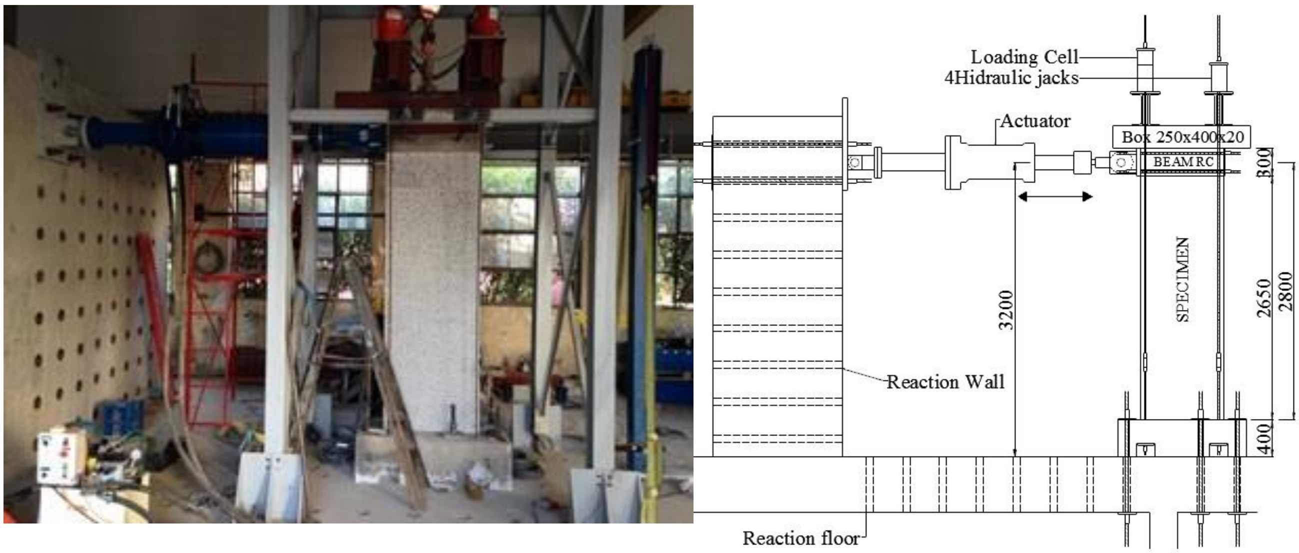

Fig. 4 - Test assembly and scheme

Materials

Typical concrete and steel materials used in Chile were considered for the tests. Concrete quality was H30 (f'_c = 25MPa - nominal), reaching strength of 33.2 MPa, 40.3MPa, 36.2MPa and 38.3MPa at the time of tests W1, W2, W3 and W4, respectively. The steel bars used are reinforcement quality A630-420H similar to grade 60 (f_y = 420 MPa - nominal). The average yield stress was 490MPa and the ultimate strength reached 670MPa.

Data acquisition

Different tools are used in all walls to measure strain or displacements. 14 strain gages are located in the reinforcing bars, most of them located at the base of the boundary longitudinal bars, and others placed on the horizontal reinforcement closet to the wall base. In addition, on the concrete surface LVDTs are installed both vertically and diagonally, in order to capture flexural and shear components of deformation, as well as, top displacement and any pedestal movement. They varied between 25 and 32 sensors. Finally, photogrammetry is used to monitor global and local (discontinuity region) displacements and strains of the walls.

Load versus displacement response and overall behavior

All specimens were tested under the same conditions, both axial load and lateral displacement, besides of having the same reinforcement scheme, differing only by the level of discontinuity at the base. Thus the capacity of the wall is similar in all 3 specimens (W1, W2, W3), but not in the location and concentration of damage, since the arrangement of type flag wall, creates a strain concentration at the base, which is appreciable at large drift levels (4%).

Figures 5, 6 and 7 show the response of the specimens tested under lateral cyclic loading, showing the lateral load versus lateral displacement. Lateral displacement was determined at the location of the actuator, and corrected by the pedestal sliding and rotation. For all tests cycles were started in the negative direction, where negative direction is toward the reaction wall (towards the left side in the figures). For all specimens the first yield was estimated according to the equations proposed by Ahumada [2]. The response for each of the performed tests is described in the following sections.

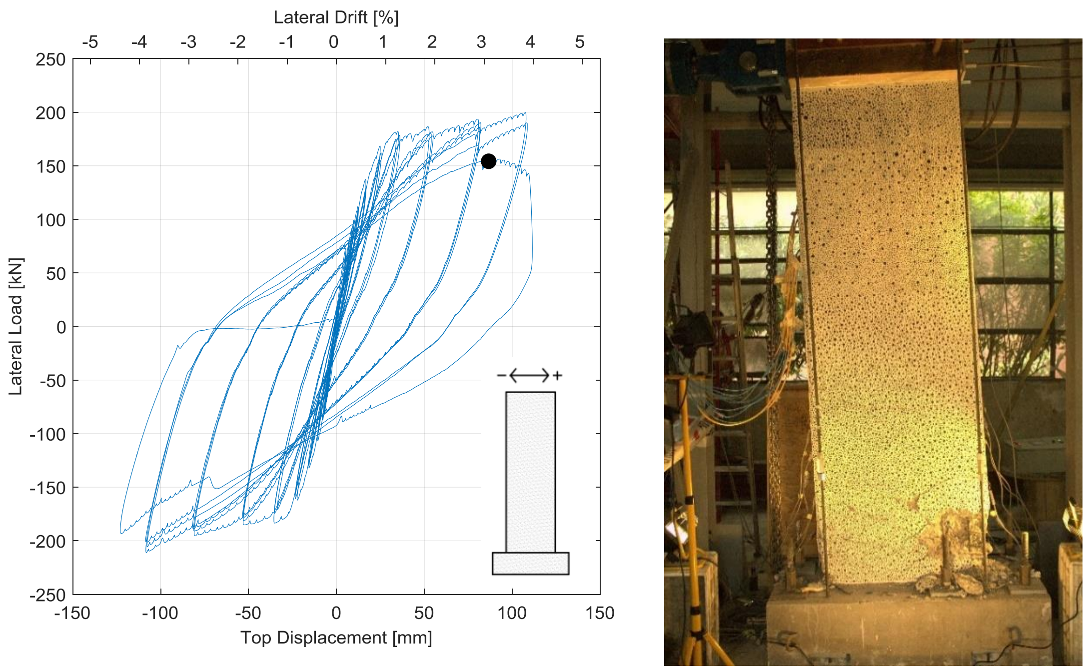

Fig. 5 - Lateral load vs top displacement and fracture Specimen 1

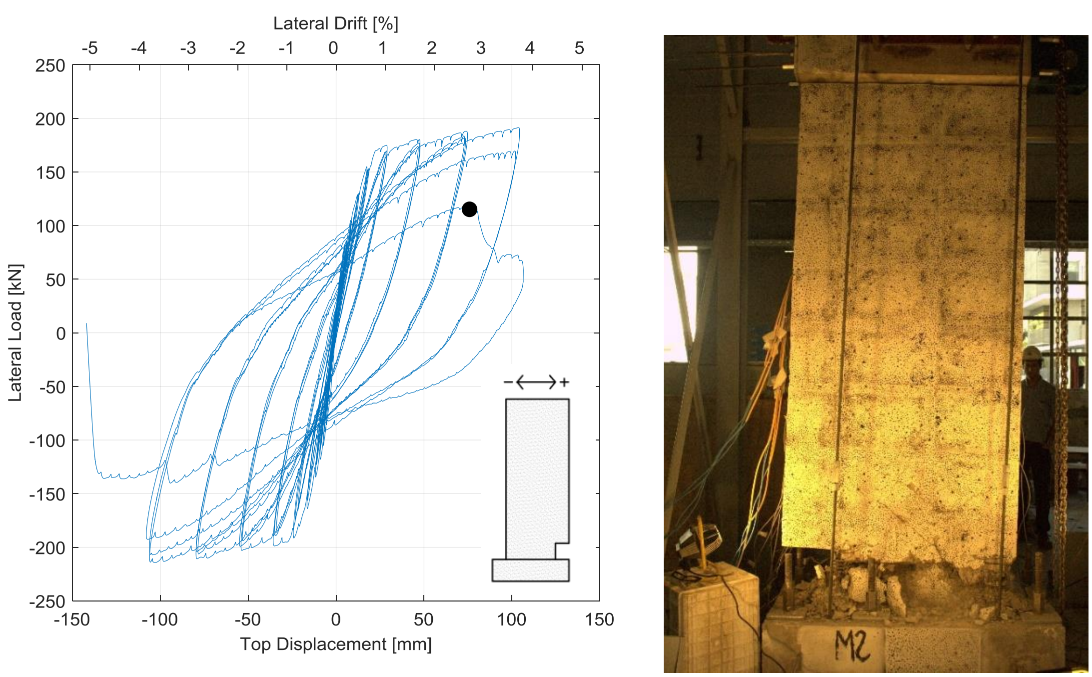

Fig. 6 - Lateral load vs top displacement and fracture Specimen 2

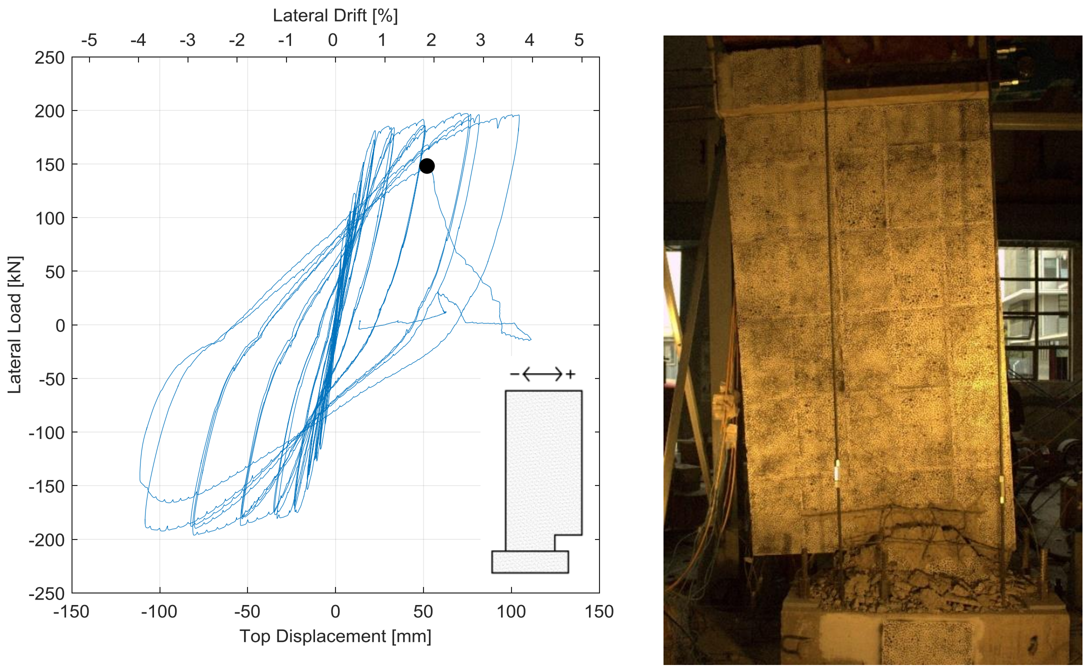

Fig. 7 - Lateral load vs Top displacement and fracture Specimen 3

Specimen W1: Initial stiffness of the wall is similar for both directions. The first cracks that can be distinguished on the wall occurred in the third cycle of 0.3% drift in the negative direction at the bottom of the wall. Further cycles, increase the number of cracks and widen them. In the first cycle of 3% drift in the negative direction, the wall begins to lose concrete cover at the wall boundaries, and diagonal cracks extended beyond half of the height of the wall. Finally strength degradation occurred in the third cycle of 4% drift in the positive direction, where the boundary bars present buckling and concrete at the wall edges is crushed. However, the test was pushed towards the 6% drift level in the negative direction, but was stopped at a drift of 4.5% since the specimen was unstable.

Specimen W2: Shows a similar behavior to the specimen W1, especially at the early stages. The first cracks that can be distinguished on the wall occur in the first cycle of 0.3%, which is earlier than in W1. In the first cycle of 3% drift in the negative direction, the wall begins to lose concrete cover, which is notably on the side of the discontinuity. Diagonal cracks are also extended over half the height of the wall, although concentrated at the wall bottom. Finally, strength degradation occurs during the third cycle of 4% drift in the positive direction, where the bars are exposed and suffer considerable buckling, while concrete at the wall edges has crushed. Also, edge reinforcement of positive side were fractured. Even though load was applied in the positive direction it was stopped since concrete and steel deterioration maintaining a degraded strength of the wall and further damage was observed, including bar fracture.

Specimen W3: Similar behavior is observed in this specimen as with the other two. The first cracks that can be distinguished on the wall occur in the first cycle of 0.3% in the negative direction, concentrated at the bottom of the wall. Similar to the specimen W2, the first yield is achieved before the base case (W1) did. In the second cycle of 3% in the positive direction, the wall begins to lose concrete cover, mostly at the wall boundary near the discontinuity region. Diagonal crack are observed above half the wall height. Finally, strength degradation occurs in the second cycle of 4% drift in the positive direction, presenting longitudinal bar buckling and concrete crushing at wall ends. The second cycle at 4% was not completed since bars fracture and strength degraded rapidly.

Photogrammetry

The first three specimens described are analyzed in this document. Figures 8, 9 and 10 expose the strain fields at 2% and 3% drift in both directions. Principal tensile strain is shown in all figures, with identical color scale. The software used to measure strain with photogrammetry is Ncorr [7, 8], which is and open source software able to calculate displacements and strains in horizontal and vertical directions.

The first one (W1) has a rectangular form and it is the reference specimen. At 2% to drift (fig.8 a-b), is possible to observe that the strains reach symmetric magnitude and distribution in height, where at the bottom of the wall the biggest strains are reached. At 3% to drift (fig.8 c-d), strain is distributed in a longer height than for 2% drift. In addition, the strains reduces importantly after a height of length l_w.

Second and thirds (Figs. 9 and 10) specimen have a slightly different behavior because larger strain values are observed at less than l_w, with an important concentration of strain at a higher location when going in the negative direction attributed to the end of the boundary reinforcement at the discontinuity region (Figs. 9a,c and 10a,c). The strain field is distorted at such location.

Despite that, the cracks are concentrated on base of wall, specifically where the opening has started. Positive and negative directions are different regarding crack distribution, which can be observed with light blue color. Positive directions always show less cracks in the upper section of the wall.

In general, at 2% and 3% drift, strains show the biggest concentration of tension in the opening edge for positive loading direction (Figs. 9b,c and 10b,d). Direction of cracks are diagonals and point to the opening (when walls are pushed to left).

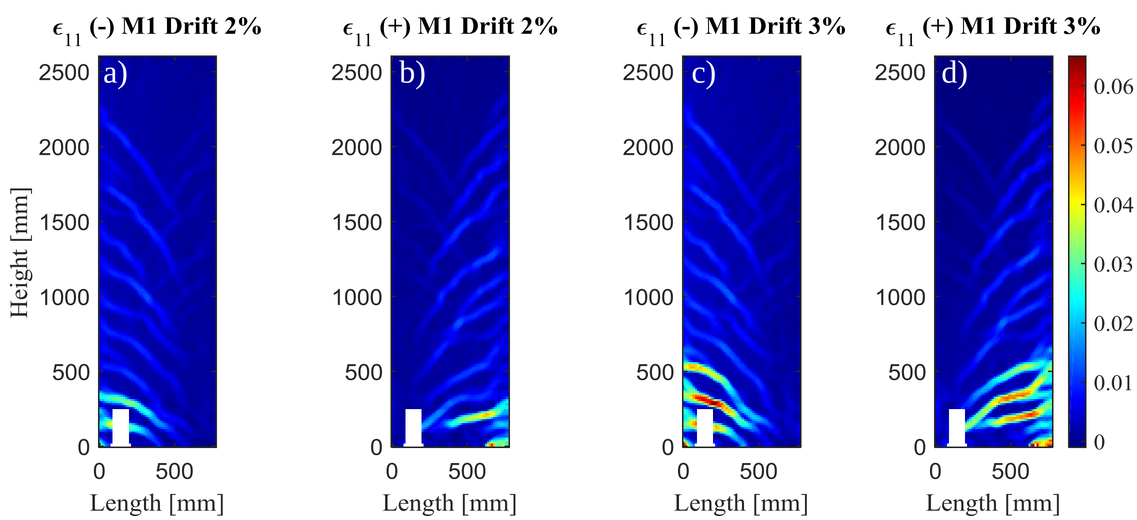

Fig. 8 - Principal strain Specimen 1 by photogrammetry: (a-b) 2% drift; (c-d) 3% drift

Santiago Chile, January 9th to 13th 2017

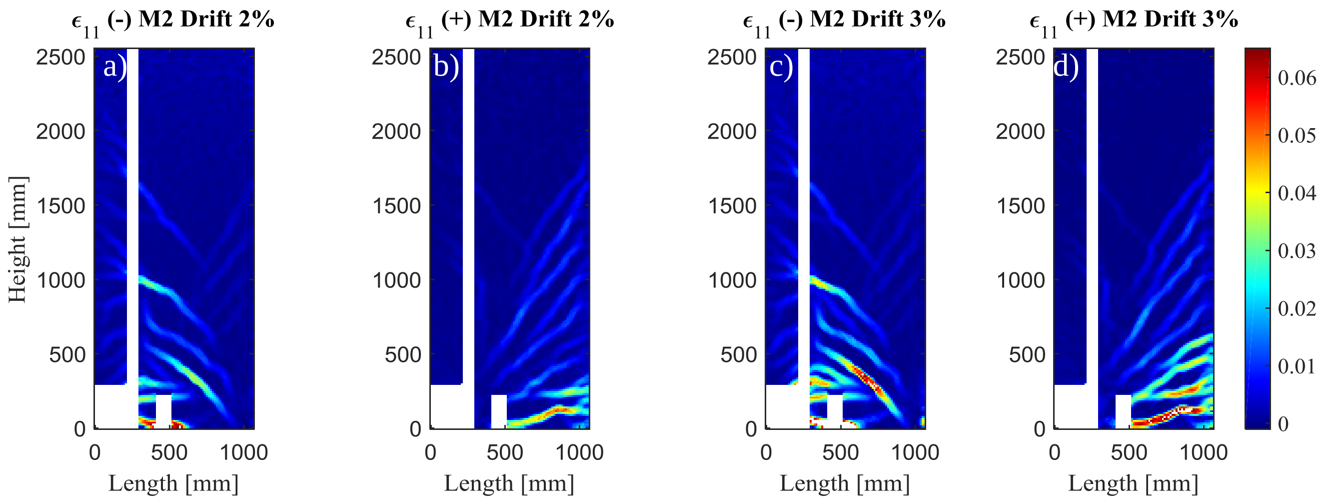

Fig. 9 - Principal strain Specimen 2 by photogrammetry: (a-b) 2% drift; (c-d) 3% drift

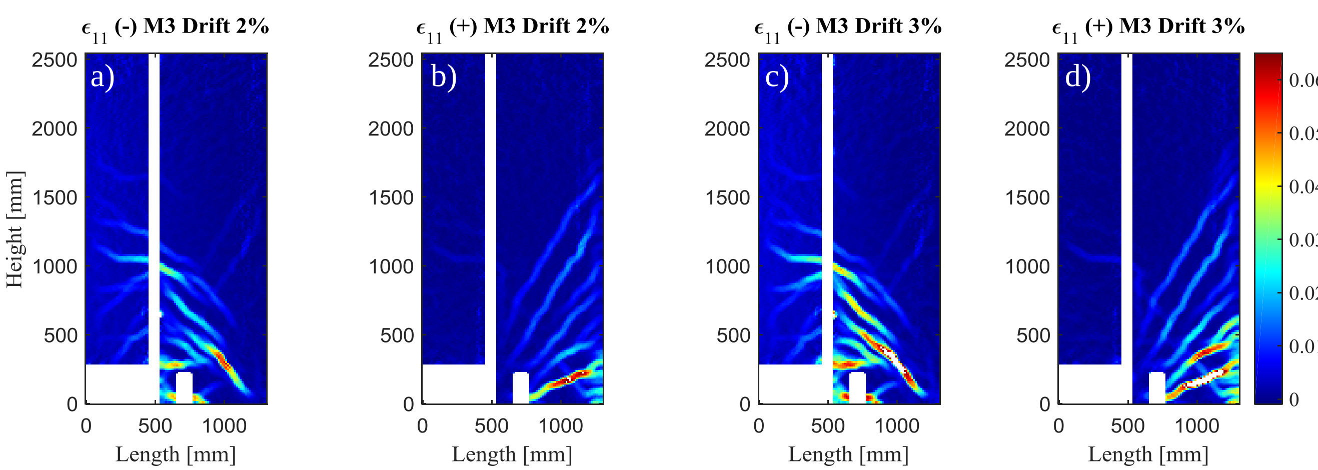

Fig. 10 – Principal strain Specimen 3 by photogrammetry: (a-b) 2% drift; (c-d) 3% drift

Figure 11 shows vertical strain on most extreme tensile fiber of specimen W1, W2 and W3. Left and right half correspond to left and right edge when they are stretched, respectively, which is consistent with the loading direction. In the case of specimens W2 and W3, the negative direction considers the strain at the same location as specimen W1, that is, where the wall base is discontinuous. Fig. 11(a) shows a symmetric behavior with a strain concentration at the base for W1. Starting at 1.35% drift, an abrupt increase of strain is detected. That behavior is attributed to lengthen of the plastic hinge. At larger levels of drift, the plastic hinge reaches a higher height. At 1.35%, 2% and 3% drift levels; the height of plastic hinge reaches approximated values of 200mm, 450 mm and 700 mm, respectively. This increment in plastic hinge length is consistent with Massone et al. [1], where the plastic hinge length increases with the plastic drift level. Specimens W2 and W3 (Fig. 11b,c) show a similar behavior in the positive side of the plot, which means that the continuous edge is in tension. The strain magnitude and distribution is similar to specimen W1. The negative direction shows a different behavior, with a more pronounced concentration of strain at the wall base with a peak strain value at the beginning of the discontinuity (300mm). Another important feature is the large strain value observed at the location of the end of the discontinuous longitudinal reinforcement (1000mm).

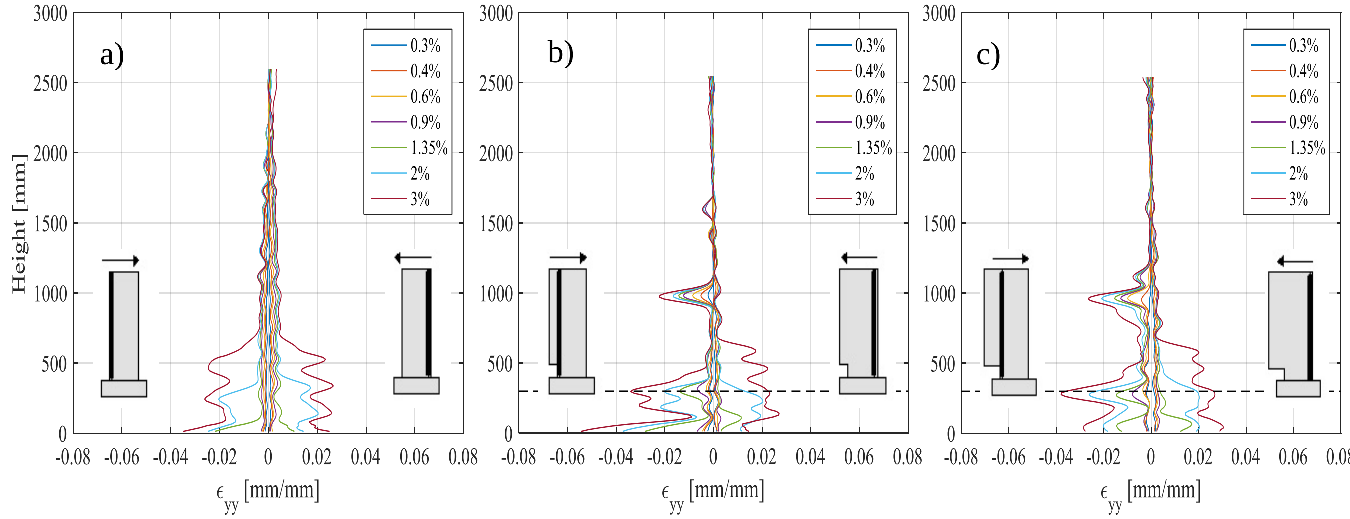

Fig. 11 - Tensile vertical strain on extreme fiber at different drift levels for specimen: (a) W1, (b) W2, and (c) W3.

Conclusions

Walls with discontinuities as setback (flag-wall) are common in Chile, but little information on their behavior is available. Ahumada [2] presents predictive estimation of yield displacement, plastic hinge length and base curvature, based on a fiber model that includes setback at the wall base (flag-wall) as an extension of the work by Massone et al. [1]. In general, the plastic hinge located at the base increases in height as it increases the level of wall top displacement. In the case of rectangular walls, the curvature gradually increases in height, whereas in walls with the presence of discontinuity (setback) at the base, the plastic hinge tends to concentrate at the base.

This work presents experimental data on walls with setback discontinuities (flag-wall). Four specimens are constructed, where one of them has rectangular cross-section and the others have an opening at the base, representing a flag wall. They are anchored to a floor reaction, applying on them a constant axial force of 0.1f'cAg and a cyclic lateral loading. Specimen W4 is not shown in this article.

All specimens show a similar load versus top displacement response, where degradation is always observed after reaching the first cycle of 4% drift. The rectangular specimen (W1) strength degradation starts in the thirst cycle of 4% drift in the positive direction, although it was possible to push it up to 4.5% in the opposite direction, presenting buckling of longitudinal bars and concrete crushing. Specimen W2 has degradation on the second cycle of 4% drift in the positive, presenting longitudinal bar buckling and fracture. Specimen W3 also presented degradation on the second cycle of 4% drift.

Analysis by photogrammetry is realized as well, which is shown as the principal tensile strain at two drift levels. In specimen W1, largest strains are observed at the wall bottom, but important strain are also observed almost over the entire wall height. For walls with openings (W2 and W3) when loaded in the positive direction, important strains are limited to the bottom of the wall, close to the height of the discontinuity. In the negative direction, there is important tensile strain at the end of the longitudinal reinforcement that is discontinuous above the opening. This results and the initiation of strength degradation indicate that the discontinuity concentrated the damage closer to the base of the wall, forcing the degradation to occur in an earlier displacement, although for the same cycle.

Finally, tensile vertical strains over height for specimen W1 are analyzed at different drift levels. Larger drift levels increases the plastic hinge length consistently, where large strains are only observed after reaching a drift level of 1.35%.

Acknowledgements

This work was financially supported by FONDECYT regular 2013 N°1130219 "Analytical and experimental study of RC walls with discontinuities". Also, the help with the specimens testing by Ernesto Inzunza, Victor González and Pedro Soto are also thanked.

References

[1] Massone L, Alfaro J, Ahumada M, Rojas F (2015): "Lateral displacement and curvature estimation in slender walls" (in Spanish), N°29, XI Congreso Chileno de Sismología e Ingeniería Sísmica ACHISINA 2015.

[2] Ahumada M (2014): "FEM modeling of slender RC walls with discontinuities at the base. Design recommendations" (in Spanish). Civil Engineering thesis, University of Chile.

[3] Rojas F (2012): "Development of a nonlinear quadrilateral layered membrane element with drilling degrees of freedom and a nonlinear quadrilateral thin flat layered shell element for the modeling of reinforced concrete walls", PhD Dissertation, University of Southern California, Los Angeles, California.

[4] Taylor C, Cote P, Wallace J (1998): "Design of Slender Reinforced Concrete Walls with Openings", Technical Paper Title no. 95-S39, ACI Structural Journal, V 95 No. 4, pp. 420-433.

[5] Ali A, Wight J (1990): "Reinforced Concrete structural walls with staggered opening configurations under reverse cyclic loading", Report No. UMCE 90-05, Department of civil engineering, University of Michigan, Ann Arbor, Michigan.

[6] ACI T1.1-01, (2001), "Acceptance Criteria for Moment Frames Base on Structural Testing", American Concrete Institute, ACI ITG/T1.1-99.

[7] Blaber J, Antoniou A (2015): "Ncorr: Instruction Manual", Georgia Institute of Technology, Version 1.2.1.

[8] Blaber J, Adair B, Antoniou A (2015): "Ncorr: Open-Source 2D Digital Image Correlation Matlab Software, Experimental Mechanics, DOI: 10.1007/s1134-015-0009-1, Society for Experimental Mechanics 2015.